



# Hydrocracking reaction pathways of 2,6,10,14-tetramethylpentadecane model molecule on bifunctional silica–alumina and ultrastable Y zeolite catalysts

G. Burnens<sup>a</sup>, C. Bouchy<sup>b</sup>, E. Guillon<sup>b</sup>, J.A. Martens<sup>a,\*</sup>

<sup>a</sup> Centre for Surface Chemistry and Catalysis, K.U. Leuven, Belgium

<sup>b</sup> IFP Energies nouvelles, Direction Catalyse et Séparation, Rond-point de l'échangeur de Solaize, BP 3, 69360 Solaize, France

## ARTICLE INFO

### Article history:

Received 19 April 2011

Revised 27 May 2011

Accepted 5 June 2011

Available online 14 July 2011

### Keywords:

Hydrocracking

Terpenoid alkanes

Pristane

$\beta$ -Scission

Reaction kinetics

## ABSTRACT

Pristane (2,6,10,14-tetramethylpentadecane) was used as a model molecule for investigating the hydrocracking reaction pathways of a large tetramethylbranched alkane. Pristane was hydroconverted in a vapor phase continuous flow laboratory reactor over Pt/SiO<sub>2</sub>–Al<sub>2</sub>O<sub>3</sub> and Pt/US–Y zeolite catalysts. On the two catalysts, pristane underwent methyl shift and hydrocracking. The zeolite altered the four methylbranching positions, while the silica–alumina favored methyl shift of the inner methyl groups. The cracked products were analyzed in terms of carbon numbers and branchiness. The pristane hydrocracking patterns obtained on the silica–alumina and the zeolite catalyst were similar. The study revealed that the cracking proceeded on tetrabranched positional isomers of the pristane molecule. From the preferential formation of specific fragments and the suppression of others, it was deduced that rival  $\beta$ -scission reactions occurred at significantly different reaction rate. Carbon–carbon bonds next to inner branchings were preferentially cracked. This is an important difference with shorter alkanes in which reactions of a same type occur at a same rate. The present observation implies that kinetic models established for short alkanes do not apply to heavy multibranching alkanes. A new paradigm will be needed for modeling hydrocracking of multibranching heavy alkanes.

© 2011 Elsevier Inc. All rights reserved.

## 1. Introduction

Hydrocracking is an established petroleum refining process. Traditionally, heavy petroleum fractions serve as feedstock of a hydrocracker unit to produce a range of products, including LPG, gasoline, diesel, kerosene, and lubricant bases [1,2]. A more recent application is hydrocracking of very long *n*-alkanes produced in Fischer Tropsch (FT) processes running in wax mode for producing diesel range product [3–7]. Algae based hydrocarbons might also become a major feedstock for hydrocracking processes [8,9]. Very relevant hydrocarbons from C<sub>20</sub> to C<sub>40</sub> are, e.g., contained in Botryococcus algae oil [10,11].

Hydrocracking is performed over a bifunctional catalyst in the presence of hydrogen. The catalytic chemistry of hydrocracking reactions of relatively short *n*-alkanes up to *n*-C<sub>17</sub> over the popular bifunctional ultrastable Y zeolite (Pt/US–Y) representative of a catalyst without shape selectivity effects has been investigated in numerous studies and is fairly well understood [12–17]. In the reaction scheme of hydrocracking of *n*-alkanes, the actual scission of the molecule is preceded by skeletal branching. Hydrocracking proceeds through  $\beta$ -scission of alkylcarbenium ions derived from

the saturated molecules via dehydrogenation over the metal function of the catalyst and protonation of the double bond on Brønsted acid sites [12,17]. The reaction rate of  $\beta$ -scission is dependent on the type of alkylcarbenium ions involved and reflects the dependence of the stability of alkylcarbenium ions on the inductive effect of alkyl substituents (Fig. 1).  $\beta$ -scission reactions starting from a secondary alkylcarbenium ion of a linear hydrocarbon chain lead to a shorter primary alkylcarbenium ion and an alkene (type D, sec → prim) and are very slow. Faster are the scissions converting a secondary ion into another secondary ion (type C, sec → sec) requiring at least one branching in the hydrocarbon chain.  $\beta$ -scissions involving tertiary ions and secondary ion (type B<sub>1</sub>, sec → tert) and B<sub>2</sub>, tert → sec) require at least two branchings and are faster. The fastest  $\beta$ -scission converts a tertiary alkylcarbenium ion into a shorter tertiary ion and an alkene (type A, tert → tert) and acts on tribranched hydrocarbon chains with specific branching positions. Thus, the sensitivity to cracking increases with increasing number of branchings in the hydrocarbon chain [17].

In addition to differences in reaction rate, the branchiness of the cracked products is dependent on the type of hydrocracking. On alkanes with three branchings type A hydrocracking leads to branched cracked products. Type B<sub>1</sub> and B<sub>2</sub> hydrocracking of dibranched alkanes lead to branched as well as linear cracked products while type C hydrocracking of monobranched alkanes

\* Corresponding author.

E-mail address: [Johan.Martens@biw.kuleuven.be](mailto:Johan.Martens@biw.kuleuven.be) (J.A. Martens).

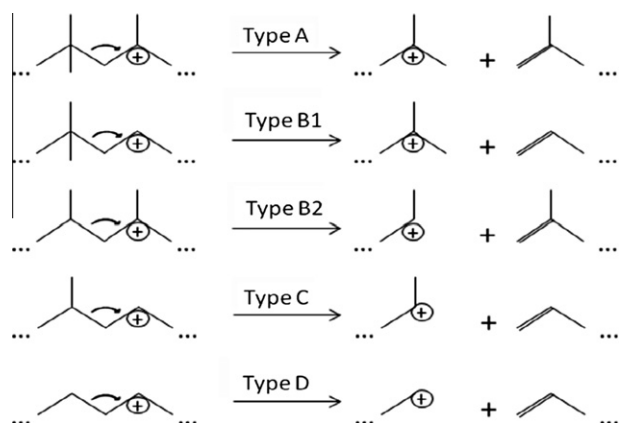


Fig. 1. Hydrocracking modes via  $\beta$ -scission [17].

and D hydrocracking of linear alkanes yield linear fragments only (Fig. 1). Evidently, the branchiness of the cracked products obtained via the same mechanisms acting on isoalkanes with higher number of branchings than necessary for the  $\beta$ -scission will be higher.

Most of the experimental research on hydrocracking of model alkanes has been conducted using *n*-alkanes. The skeletal isomerization of an *n*-alkane chain is a sequential process introducing one branching at the time [18–21]. Linear chains are little sensitive to cracking because the only available reaction pathway is the energetically unfavorable type D  $\beta$ -scission. Monobranched alkyl chains are susceptible to type C hydrocracking, dibranched chains to type B<sub>1</sub>, B<sub>2</sub>, and C depending on the relative positions of the branchings. Tribranched chains offer an additional fast type A  $\beta$ -scission, provided the three branchings are located at  $\alpha, \gamma, \gamma$  relative positions with respect to the positively charged C atom (Fig. 1).

Branching of alkane chains occurs via protonated alkylcycloalkane intermediates [11,15]. According to alkylcarbenium ion chemistry except for the C<sub>2</sub> and C<sub>*n*-2</sub> positions that are less favorable for formation of a branching, there is no positional selectivity and branching can be generated anywhere in an alkane chain [11]. The formation of a side chain results in a shortening of the main chain with the number of carbon atoms contained in the side chain. Very specific configurations of side chains and positive charge need to be accomplished for type B<sub>1</sub>, B<sub>2</sub>, and A hydrocracking (Fig. 1). They are reached by hydride and alkyl shifts. The order of relative reaction rates of alkylcarbenium ions obeys the order [12]:

type A  $\beta$ -scission > alkyl shift  
 > type B<sub>1</sub>, B<sub>2</sub>, C  $\beta$ -scission and branching  
 >> type D  $\beta$ -scission

In *n*-decane hydrocracking over Pt/US-Y zeolite, type A hydrocracking contributes ca. 69% of the hydrocracked products, B<sub>1</sub> and B<sub>2</sub> mechanisms ca. 18%, and type C hydrocracking 13% [22]. These relative contributions are little dependent on reaction conditions [23]. In the hydrocracking of the series of model *n*-alkanes from *n*-C<sub>10</sub> to *n*-C<sub>17</sub>, the contribution of type B<sub>1</sub> and B<sub>2</sub> hydrocracking is increased a little at the expense of type A. This change has been interpreted by the increasing number of alkyl shifts that are required to gather far apart branchings to reach the configuration for a type A scission in comparison with the B type scissions which are demanding adequate positioning of only two branchings, or type C operating next to any branching [24].

Few studies have dealt with hydrocracking of branched alkanes with 10 or more C atoms (Table 1). The hydroconversion of the










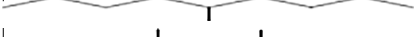
individual methylnonane positional isomers and of selected dimethyloctanes on Pt/US-Y zeolite has been investigated [20]. In the conversion of these model molecules, there is substantial skeletal isomerization preceding the actual cracking. Hydrocracked product distributions obtained from these monobranched and dibranched C<sub>10</sub> isomers were similar to the one obtained from *n*-decane, showing that alkyl shifts were sufficiently rapid to scramble the internal distribution of positional isomers. The initial methylbranching position in a monobranched or dibranched C<sub>10</sub> molecule does not matter to the final cracked product distribution. Deviation from the common hydrocracking pattern was obtained in the hydrocracking of 3,3,5-TMC<sub>7</sub> (3,3,5-trimethylheptane) and 2,4,6-TMC<sub>7</sub>. With these tribranched model molecules, the contribution of type A hydrocracking was significantly larger than with less branched molecules (Table 1). In 3,3,5-TMC<sub>7</sub> molecule, the methyl groups are in a favorable position for type A hydrocracking leading to isopentane. In 2,4,6-TMC<sub>7</sub> after two methyl shifts, 2,4,4-TMC<sub>7</sub> isomer can be obtained which is prone to type A hydrocracking and formation of isobutane and 2-methylpentane.

Thybaud et al. described hydrocracking using a single-event microkinetic model (SEMK) involving a detailed description of the physisorption and chemisorption as well as the elementary reaction steps alkylcarbenium ions undergo on a Pt/US-Y zeolite [25]. Hydrocracking of *n*-C<sub>12</sub> and the tribranched skeletal isomers 4,4,6-TMC<sub>9</sub> and 2,5,8-TMC<sub>9</sub> in a fixed bed reactor were simulated [25]. Hydrocracking of 4,4,6-TMC<sub>9</sub> resulted selectively in branched C<sub>6</sub> fragments, as expected for a molecule suitable for type A hydrocracking. Interestingly, the cracked product distribution obtained from 2,5,8-TMC<sub>9</sub> changed significantly with conversion. At very low conversion, the simulation revealed the two possible type C hydrocracking events on the original isomer to occur leading to C<sub>3</sub> + *i*-C<sub>9</sub> and *i*-C<sub>5</sub> + *i*-C<sub>7</sub> products (Table 1). At high conversion, the branching positions were changed by skeletal isomerization, and type A hydrocracking became dominant.

Molecular aspects of hydrocracking of still longer branched alkane chains have not yet been investigated in great detail. A scientific question remaining unanswered is till what distance two side chains on a very long alkane chain will still be shifted closer to each other by a sequence of alkyl shifts to relative positions suitable for B<sub>1</sub> or type B<sub>2</sub> hydrocracking. The same question can be put forward for the type A hydrocracking necessitating the shifting of three side chains to reach the suitable configuration. The question is important since the location of the cracked carbon–carbon bond along the chain matters to the molecular weight of the fragments and the petrochemical fraction the products will belong to.

Kinetic studies with very long branched model molecules are needed to investigate the impact of the distance between branchings on hydrocracking selectivity. Relevant model molecules are available. Pristane (2,6,10,14-tetramethylpentadecane) and phytane (2,6,10,14-tetramethylhexadecane) are natural saturated diterpenoid alkanes available, e.g., in shark liver oil. The phytyl moiety (2,6,10,14-tetramethylhexadecyl) is part of many organic molecules of biological importance. Molecules like pristane are relevant to industrial hydrocracking processes since they are contained in renewable hydrocarbons in microalgae and in crude oil [26,27]. Squalane (2,6,10,15,19,23-hexamethyltetracosane) is another multibranching alkane obtained by hydrogenation of the triterpenoid squalene molecule. Literature on hydrocracking of these large multibranching model alkanes is limited. Taylor and Petty investigated the hydroisomerization of a mixture of hexadecane and pristane in order to evaluate the *n*-alkane hydroisomerization activity of 10-ring zeolite catalysts in the presence of a multibranching alkane [28]. de Jong et al. investigated hydrocracking of squalane in order to reveal the enhanced accessibility of active sites in Y zeolite crystals with trimodal porosity [29]. Valéry et al. developed a kinetic model for hydrocracking of squalane

**Table 1**  
Literature data on hydrocracking of long branched model alkane molecules [13,21,22,25].

Carbon number	Model molecule	Hydrocracking products	Research approach <sup>a</sup>	
10		2-MC <sub>9</sub>	Similar as with <i>n</i> -C <sub>10</sub>	E
		3-MC <sub>9</sub>		
		4-MC <sub>9</sub>		
		5-MC <sub>9</sub>		
10		2,6-DMC <sub>8</sub>	Similar as with <i>n</i> -C <sub>10</sub>	E
		3,5-DMC <sub>8</sub>		
10		2,4,6-TMC <sub>7</sub>	Preferential <i>i</i> -C <sub>4</sub> + <i>i</i> -C <sub>6</sub> formation <i>i</i> -C <sub>5</sub> strongly favored	E
		3,3,5-TMC <sub>7</sub>		
12		2,5,8-TMC <sub>9</sub>	C <sub>3</sub> + <i>i</i> -C <sub>9</sub> and <i>i</i> -C <sub>4</sub> + <i>i</i> -C <sub>8</sub> formation at low conversion preferential <i>i</i> -C <sub>6</sub> formation till 40% conversion	M
		4,4,6-TMC <sub>9</sub>		

<sup>a</sup> Experiment (E) or modeling (M).

and computed the molar repartition of cracked products by carbon number [30]. The simulated cracking product pattern was monomodal with a shallow maximum around C<sub>7</sub>. Interestingly, the experimental cracked product distribution those authors provided showed discrete minima at C<sub>7</sub>, C<sub>12</sub>, C<sub>18</sub>, and C<sub>22</sub> but the origin of those was not discussed.

In this work, we report detailed hydrocracking patterns of the tetrabranched model molecule pristane on two industrially relevant bifunctional catalysts: ultrastable Y zeolite (Pt/US-Y) and silica–alumina (Pt/SiO<sub>2</sub>–Al<sub>2</sub>O<sub>3</sub>). The purpose of the work was to reveal the hydrocracking pathways of a molecule presenting a large number of chain branching at distant relative positions.

## 2. Experimental

### 2.1. Catalysts

Silica–alumina catalyst with supported Pt (Pt/SiO<sub>2</sub>–Al<sub>2</sub>O<sub>3</sub>) was supplied by IFP Energies nouvelles. The ultrastable Y zeolite was a commercial sample with code name CBV-760 (PQ Corp.). Platinum was loaded via incipient wetness impregnation method using aqueous solution of [Pt(NH<sub>3</sub>)<sub>4</sub>]Cl<sub>2</sub>. The nominal Pt content on dry weight basis was 0.5 wt.% for Pt/US-Y zeolite and 0.6 wt.% for Pt/SiO<sub>2</sub>–Al<sub>2</sub>O<sub>3</sub>. Pt/USY catalyst powder and Pt/SiO<sub>2</sub>–Al<sub>2</sub>O<sub>3</sub> extrudates were, respectively, compressed and crushed and sieved into pellets of 0.25–0.50 mm diameter and loaded in the reactor tube with internal diameter of 1 cm and a length of 20 cm. The catalyst bed comprised from 0.2 to 1.6 g of catalyst pellets. The in situ pretreatment procedure comprised heating under O<sub>2</sub> to 400 °C and subsequently isothermally during 1 h, flushing of the line with N<sub>2</sub> and reduction with H<sub>2</sub> without intermittent cooling during 1 h. The platinum dispersion on the Pt/US-Y and Pt/SiO<sub>2</sub>–Al<sub>2</sub>O<sub>3</sub> determined via H<sub>2</sub>/O<sub>2</sub> titration was 16% and 60%, respectively.

### 2.2. Hydrocracking experiments

The feedstock for the reactor was made up of 1 mol% of pristane (Sigma, ≥98%) and 99 mol% of *n*-heptane (Acros Organics, >99%, pure). Experiments were made in a downstream continuous flow reactor. The hydrocarbon feed was pumped at a rate of 0.10 ml min<sup>-1</sup> into a vaporization chamber heated at 280 °C and

mixed with H<sub>2</sub> at a molar ratio of H<sub>2</sub>: hydrocarbon of 13.1 at a total pressure of 0.45 MPa. The reaction temperature was changed and reaction products sampled online after at least 1 h on stream at fixed reaction conditions. The reaction products were analyzed by online GC over an apolar capillary column (HP-1) and flame ionization detector. Analysis of cracked products was done based on previous experience with long-chain *n*-alkanes in the same reactor [31–33].

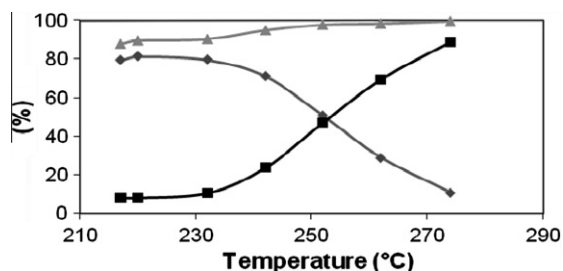
## 3. Results and discussion

### 3.1. Hydroconversion of pristane over Pt/SiO<sub>2</sub>–Al<sub>2</sub>O<sub>3</sub>

Pt/SiO<sub>2</sub>–Al<sub>2</sub>O<sub>3</sub> catalyst was loaded in the fixed bed continuous flow reactor operated under vapor phase reaction conditions. The use of a mixture of 1 mol% pristane in *n*-heptane solvent facilitated vaporization and enabled the feeding of small and stable quantities of pristane to the reactor at a relatively low overall H<sub>2</sub>/hydrocarbon molar ratio of 13.1:1. Contact time and reaction temperature range were selected in order to cover the full range of hydrocracking conversion levels. Typically, the reaction was run during 90 min at a given reaction temperature before the reaction products were sampled and analyzed online. Under the investigated reaction conditions, there was no catalyst deactivation as verified with return points to original conditions. *n*-Heptane solvent was verified to be inert on the selected catalysts under the investigated reaction conditions.

The pristane conversion and the yield of skeletal isomers and cracked products over Pt/SiO<sub>2</sub>–Al<sub>2</sub>O<sub>3</sub> are plotted against reaction temperature in Fig. 2. In the reaction temperature range 217–274 °C, the pristane conversion was high and increased from ca. 84% to 100%. At 217 °C, skeletal isomerization dominated, and the hydrocracking yield was 4.9% only. At the highest reaction temperature of 274 °C, the hydrocracking yield was 88.7%.

The molar yield of cracked products according to carbon number expressed per 100 mol of pristane cracked at different reaction temperatures is presented in Fig. 3. Note that the yield of C<sub>7</sub> cracked products from pristane hydrocracking could not be determined as these products could not be distinguished from the large amount of *n*-heptane solvent in the feed. Each carbon number frac-



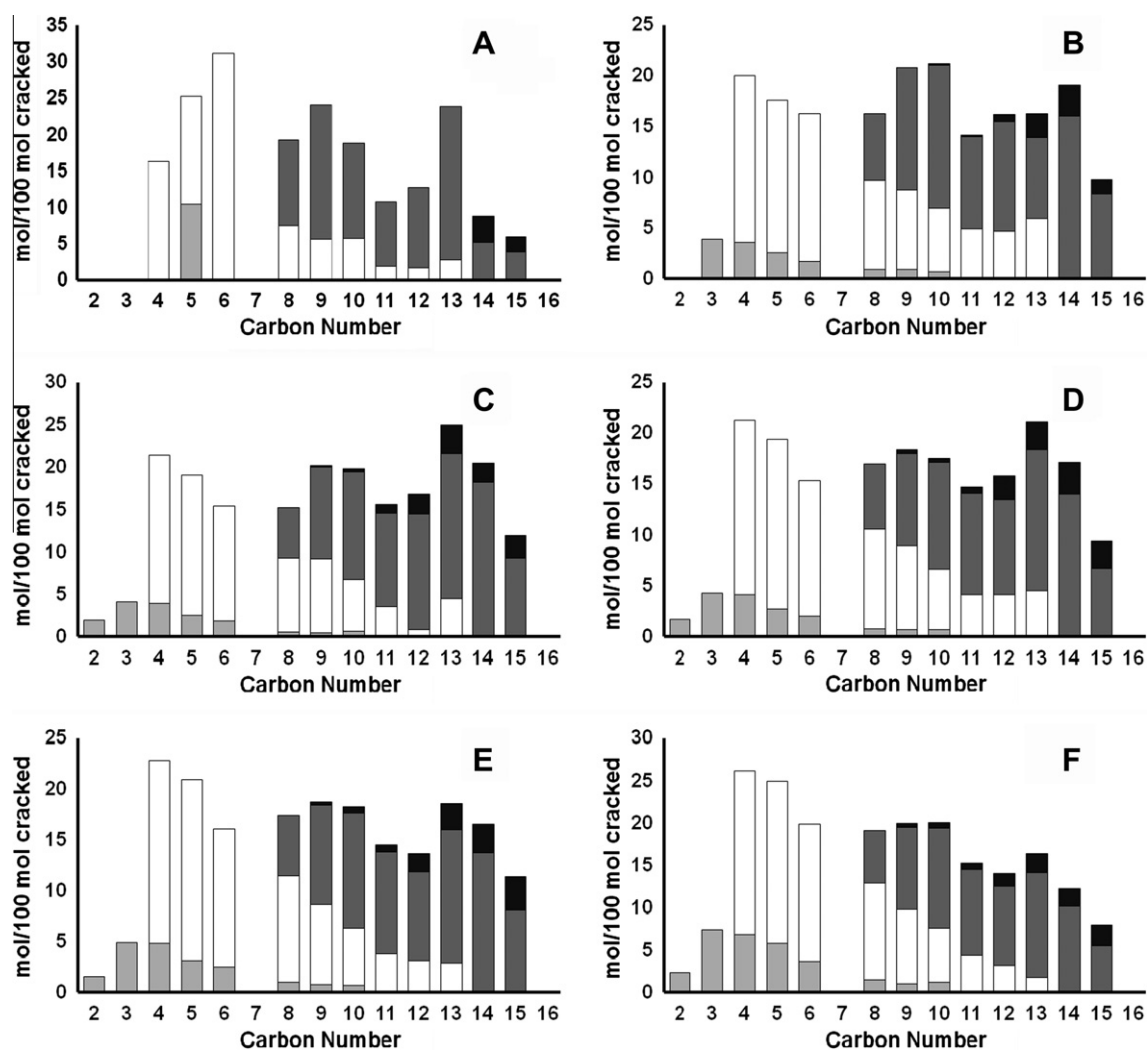
**Fig. 2.** Conversion (▲) isomerization yield (◆) and hydrocracking yield (■) versus reaction temperature in the reaction of pristane on Pt/SiO<sub>2</sub>-Al<sub>2</sub>O<sub>3</sub>.  $W/F_0$  pristane = 13,600 kg s/mol,  $P_{tot}$  = 0.45 MPa;  $P_{H_2/HC}$  = 13.1.

tion was analyzed for branchiness. At low cracking yield, some striking observations were made (Fig. 3A):

- (i) propane and C<sub>16</sub> cracked products were not formed;
- (ii) the molar yield distribution showed maxima at C<sub>6</sub>, C<sub>9</sub>, and C<sub>13</sub>;
- (iii) in the C<sub>4</sub> and C<sub>6</sub> cracked product fractions, all molecules were monobranched;
- (iv) the C<sub>5</sub> fraction contained a significant amount of *n*-C<sub>5</sub> next to *i*-C<sub>5</sub>;

- (v) the C<sub>8</sub>–C<sub>13</sub> fractions were composed of monobranched and dibranched skeletal isomers;
- (vi) the C<sub>13</sub> fraction was dominated by one specific isomer which was identified as 2,6-DMC<sub>11</sub>;
- (vii) the C<sub>14</sub> and C<sub>15</sub> fractions were composed of dibranched and tribranched isomers only.

The tetrabranched pristane molecule is susceptible to different type C hydrocracking reactions, leading to either C<sub>3</sub> + 2,6,10-TMC<sub>13</sub>, 2-MC<sub>5</sub> + 2,6-DMC<sub>11</sub>, or 2-MC<sub>7</sub> + 2,6-DMC<sub>9</sub> (Fig. 4). At low hydrocracking conversion experimentally, there was preferential formation of C<sub>6</sub> and C<sub>13</sub> fractions (Fig. 3A), which can be explained by a specific type C hydrocracking of the pristane molecule (Fig. 4B). This cracking mode gives rise to the formation of 2-MC<sub>5</sub> and 2,6-DMC<sub>11</sub>, which were observed to be the dominant molecules in these two fractions. Unexpected was that the other two possible type C β-scission reactions of pristane (Fig. 4A and C) according to the cracked product distribution (Fig. 3A) contributed less. There was no formation of C<sub>3</sub> and C<sub>16</sub> products expected to be formed according to the reaction of Fig. 4A. The formation of C<sub>3</sub> + C<sub>16</sub> fragments and of C<sub>6</sub> + C<sub>13</sub> depends from a same secondary alkylcarbenium ion and is depending on the β-scission to occur between the carbon–carbon bond next to the methyl branching at C<sub>2</sub> or C<sub>6</sub> (Fig. 4A and B). The 2-propyl cation formed in the reaction of



**Fig. 3.** Cracked product distributions from pristane on Pt/SiO<sub>2</sub>-Al<sub>2</sub>O<sub>3</sub> catalyst at different reaction temperatures. Each fraction is divided according to branchiness: light gray: linear; white: monobranched; dark gray: dibranched; black: tribranched isomers. Reaction temperature and hydrocracking yields: (A) 217 °C, 4.9%; (B) 232 °C, 10.6%; (C) 242 °C, 23.8%; (D) 252 °C, 47.0%; (E) 262 °C, 69.4%; (F) 274 °C, 89.1%. Reaction conditions of Fig. 2.



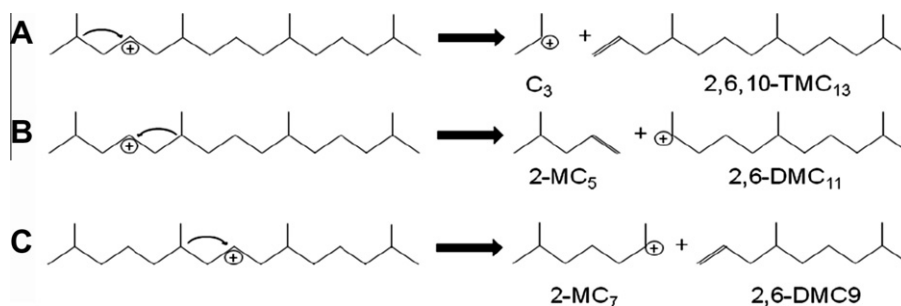


Fig. 4. Type C  $\beta$ -scission of secondary alkylcarbenium ions derived from pristane.

Fig. 4A because of lower inductive effects is less stable than the larger secondary cation leading to 2-MC<sub>5</sub>, which could explain why cracking into C<sub>3</sub> and C<sub>16</sub> fragments was disfavored compared to formation of C<sub>6</sub> and C<sub>13</sub> fragments. The suppression of C<sub>3</sub> formation was very pronounced here, and much more than expected based on earlier work on hydrocracking of smaller alkanes [14,22]. For example, in the SEMK model of hydrocracking of 2,5,8-TMC<sub>9</sub>, the formation of C<sub>3</sub> has been predicted (Table 1).

The type C hydrocracking pathway departing from a secondary alkylcarbenium ion with positive charge at the central C atom of the main chain leads to 2-MC<sub>7</sub> and 2,6-DMC<sub>9</sub> fragments (Fig. 4C). Also, this cracking pathway appeared less important, since the formation of C<sub>8</sub> and C<sub>11</sub> products was not that favored (Fig. 3A). There are no stability differences to be expected among the secondary alkylcarbenium ions needed for the experimentally preferred modes of type C hydrocracking of Fig. 4B and the suppressed mode of Fig. 4C. The observed dominance of one of the possible type C hydrocracking pathways on a same branched chain was unexpected. For shorter alkane molecules, the detailed hydrocracking patterns have been explained and modeled assuming that all hydrocracking reactions of a same type occurred at a same rate [34,35].

Analysis of the composition of C<sub>4</sub> and C<sub>5</sub> product fractions shed more light on the peculiar hydrocracking behavior of pristane on the Pt/SiO<sub>2</sub>-Al<sub>2</sub>O<sub>3</sub> catalyst at 4.9% hydrocracking (Fig. 3A). None of the type C hydrocracking reactions operating on pristane leads to C<sub>4</sub> or C<sub>5</sub> cracked products (Fig. 4). Alkyl shifts are needed to arrive at suitable branching configurations leading to cracking into C<sub>4</sub> or C<sub>5</sub> fragments. On the Pt/SiO<sub>2</sub>-Al<sub>2</sub>O<sub>3</sub> catalyst, there was substantial skeletal isomerization (Fig. 2). The reaction pathways leading to linear and branched C<sub>4</sub> and C<sub>5</sub> fragments after a minimum of methyl shifts followed by  $\beta$ -scission are presented in Fig. 5. The formation of *n*-C<sub>4</sub> from pristane can proceed in two ways, either via 1 methyl shift and type C  $\beta$ -scission (Fig. 5A) or via two consecutive methyl shifts and a type B<sub>2</sub> hydrocracking (Fig. 5B). The formation of *i*-C<sub>4</sub> necessitates 2 methyl shifts and a type B<sub>2</sub> hydrocracking (Fig. 5D). Experimentally, the C<sub>4</sub> fraction was observed to be entirely branched (Fig. 3A), meaning that the reaction pathways leading to *n*-C<sub>4</sub> did not contribute. The C<sub>5</sub> fraction contained a substantial amount of *n*-C<sub>5</sub>, although the pathways leading to linear C<sub>5</sub> fragments (Fig. 5C) are very similar to those leading to linear C<sub>4</sub> (Fig. 5A and B). The significant formation of *n*-C<sub>5</sub> in the C<sub>5</sub> fraction in contrast to the C<sub>4</sub> fraction containing no linear fragments must have another origin.

The occurrence of secondary cracking was estimated by calculating the number of moles of cracked products formed per 100 mol of pristane cracked (Table 2). At 4.9% hydrocracking, ca. 221 mol of cracked products were obtained out of 100 mol cracked pristane. An experimental value exceeding 200 mol of fragments per 100 mol of parent molecule revealed that some primary fragments underwent an additional cracking even at this low cracking conversion level. The formation of a substantial amount of *n*-C<sub>5</sub> in

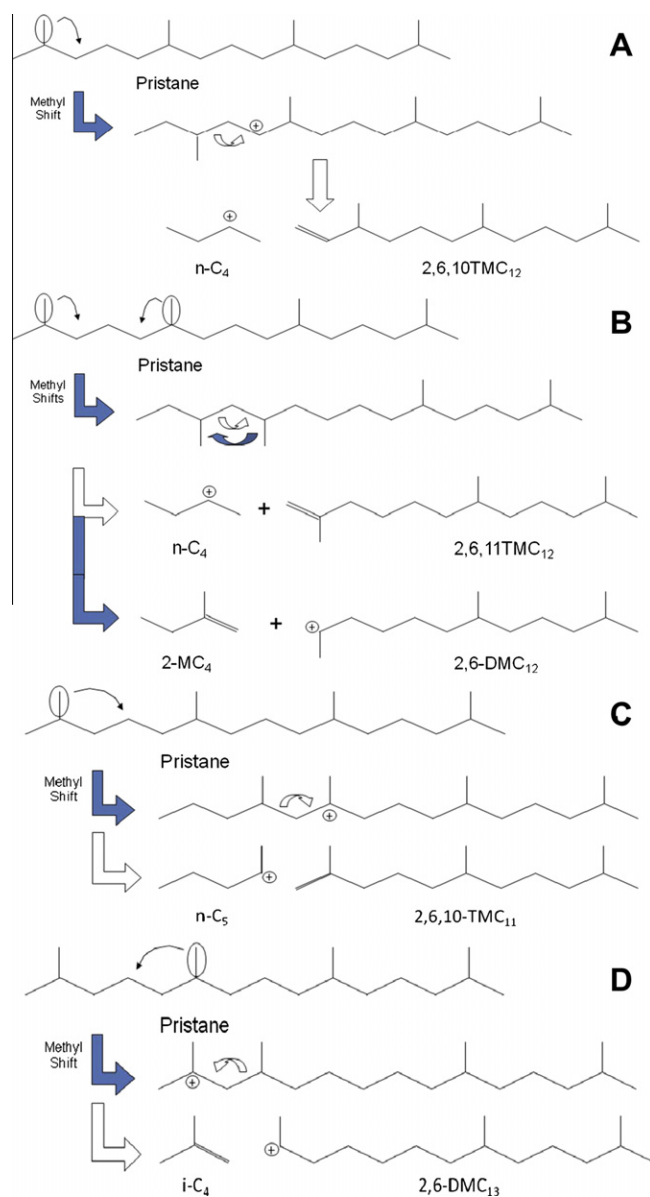


Fig. 5. Skeletal rearrangements and  $\beta$ -scission reactions leading to linear and branched C<sub>4</sub> and C<sub>5</sub> fragments after a minimum number of methyl shifts. Positive charges on alkylcarbenium ions were omitted when two possibilities are present.

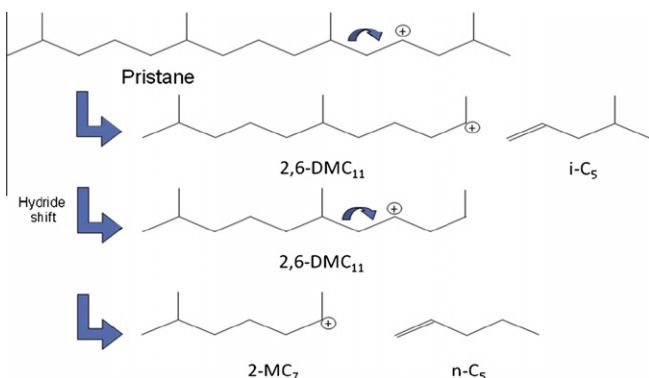
the C<sub>5</sub> fraction could be explained by secondary cracking of 2,6-DMC<sub>11</sub> molecules from the preferred primary hydrocracking pathway of Figs. 4B and 6. The abundant formation of *n*-C<sub>5</sub> and the experimentally observed molar excess of C<sub>8</sub> compared to C<sub>11</sub> frag-

**Table 2**  
Branchiness of hydrocracked products from pristane on Pt/SiO<sub>2</sub>-Al<sub>2</sub>O<sub>3</sub> catalyst.

Experimental condition	T (°C)	Hydrocracking yield		Average branchiness of cracked products	
		%	Mol/100 mol pristane cracked	Experimental	In absence of change of branchiness <sup>a</sup>
A	217	4.9	221	1.6	(1.3) <sup>b</sup>
B	232	10.6	208	1.4	1.4
C	242	23.8	211	1.4	1.4
D	252	47.0	211	1.3	1.4
E	262	69.4	214	1.3	1.4
F	274	89.1	225	1.2	1.3

<sup>a</sup> Assuming absence of changes of branchiness of pristane skeletal isomers undergoing cracking and of skeletal isomerization of cracked products.

<sup>b</sup> Substantial error because of the problematic integration of small signals in the online reaction product analysis by GC at this low hydrocracking yield.



**Fig. 6.** Secondary cracking via  $\beta$ -scission reactions explaining the formation of  $n$ -C<sub>5</sub> next to  $i$ -C<sub>5</sub> fragments at 4.9% hydrocracking conversion on Pt/SiO<sub>2</sub>-Al<sub>2</sub>O<sub>3</sub>.

ments (Fig. 3A) could be explained by this secondary cracking pathway. Thus, even at these low hydrocracking conversions, once a pristane molecule started cracking, the alkylcarbenium ion fragment underwent an additional  $\beta$ -scission.

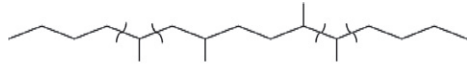
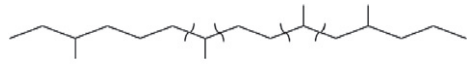
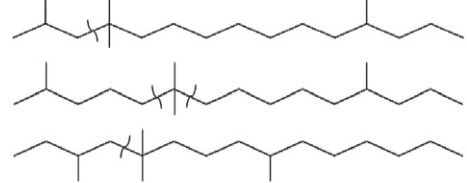
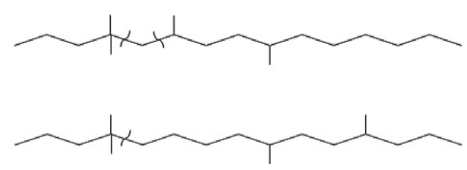
When the pristane hydrocracking conversion was increased to 10.6%, the cracked product distribution was changed substantially (Fig. 3B). Some propane was formed, and even traces of ethane. C<sub>4</sub> and C<sub>5</sub> products became more abundant compared to C<sub>6</sub>, C<sub>9</sub> and C<sub>10</sub> products were prominent, and another maximum in the cracked product distribution occurred at C<sub>14</sub> (Fig. 3B). There was less secondary cracking at 10.6% hydrocracking compared to 4.9% hydrocracking (Table 2). The branchiness of the cracked product fractions was more equally spread (Fig. 3B). The C<sub>4</sub> till C<sub>10</sub> fractions contained linear next to branched fragments (Fig. 3B). C<sub>9</sub> and heavier fractions contained tribranched next to dibranched and monobranched molecules (Fig. 3B). The cracked product composition changed only little when the hydrocracking yield was further enhanced by raising the temperature (Fig. 3C–F). Even at the highest hydrocracking conversion of 88.7%, the cracked product distribution still showed maxima at C<sub>4</sub>, C<sub>9</sub>–C<sub>10</sub>, and C<sub>13</sub> (Fig. 3F).

Cracking through  $\beta$ -scission generally leads to a loss of one side chain per scission (Fig. 1). Irrespective of branching configuration, primary cracking of the tetrabranched parent molecule is expected to result in fragments containing three branchings in total or, on average, 1.5 branchings per cracked product molecule. Secondary cracking will eliminate more branchings, causing the average branchiness to drop below 1.5. The experimental average branchiness of the cracked products at different pristane hydrocracking conversions on Pt/SiO<sub>2</sub>-Al<sub>2</sub>O<sub>3</sub> is presented in Table 2. These values were compared with the theoretical value assuming that there was no change in branchiness of parent molecules nor of fragments (Table 2). At hydrocracking levels of 10.6% and higher, the experimental branchiness of the cracked products was close to the value predicted in the absence of changes of skeletal branching degree (Ta-

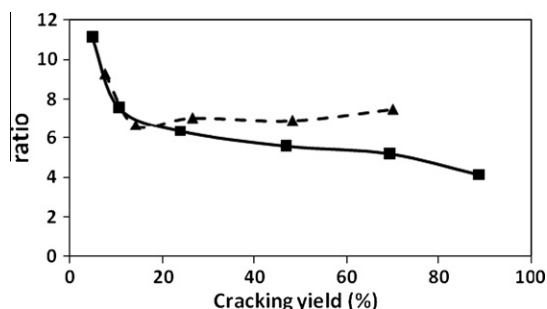
ble 2). It was concluded that the pristane molecule did not undergo substantial changes in degree of branching, but was hydrocracked either as such or after undergoing methyl shifts not altering the branchiness. At 4.9% hydrocracking, the hydrocracked products were ca. 1.6 times branched on average. This was a higher value than expected if there were no changes in branchiness, viz. 1.3. At such low hydrocracking yields because of the problematic integration of small signals in the online reaction product analysis by GC, the experimental error may be substantial. Given the agreement of experimental and theoretical value for 10.6–89.1% hydrocracking (Table 2), we ascribed the deviation at the lowest investigated cracking level to analytical inaccuracy.

Pristane is a symmetric molecule with two branchings close to the extremities of the chain (C<sub>2</sub> and C<sub>14</sub> positions), and two more centrally positioned methyl side chains at positions C<sub>6</sub> and C<sub>10</sub>. Given that the branchiness of the pristane molecule was not altered prior to the cracking (Table 2), it could be determined which of the two types of branching positions was preferentially involved in the  $\beta$ -scission reactions. In molecules with discarded branching positions, scission of carbon–carbon bonds next to an outer branching leads to the formation of a linear and a tribranched fragment (Fig. 7A). When on such molecules, the scission occurs next to one of the inner methyl groups, a monobranched and a dibranched fragment are formed (Fig. 7B). A monobranched and a dibranched fragment are obtained when the two middle methyl groups are united at a quaternary C atom (Fig. 7C). When an outer and an internal methyl group are united at a quaternary C atom, in most instances, a monobranched and a dibranched fragment are formed (Fig. 7D). Based on this analysis, the ratio of the sum of monobranched plus dibranched cracked products over linear plus tribranched cracked products could be handled to probe whether the cracking occurred next to inner or outer methyl side chains (Fig. 8). Initially, this ratio equaled 12 revealing that the cracking occurred preferentially next to inner methyl branches. The ratio dropped to ca. 7 at ca. 15% hydrocracking and decreased further to ca. 4 with increasing hydrocracking conversion. This analysis revealed branchings on a long alkane molecule not to be equivalent in hydrocracking on a Pt/SiO<sub>2</sub>-Al<sub>2</sub>O<sub>3</sub> catalyst.

A typical chromatogram of the skeletal isomers obtained by hydroisomerization of pristane on Pt/SiO<sub>2</sub>-Al<sub>2</sub>O<sub>3</sub> is presented in Fig. 9. The skeletal isomers eluted from the online capillary GC column as an envelope of overlapping peaks. The isomer presenting the largest signal in the chromatogram of Fig. 9 was a primary product observed as the main product at very low conversion. It was tentatively assigned to 3,6,10,14-TeMC<sub>15</sub> corresponding to one methyl shift on the original 2,6,10,14-TeMC<sub>15</sub>. Generally, on an apolar column, a 3-methylbranched isomer elutes later than the corresponding 2-methylbranched isomer [31,32]. Other skeletal isomerization products from pristane were arbitrarily divided into isomers eluting earlier than pristane, and isomers eluting later from the GC column (Fig. 9). The elution time of linear, monobranched, and dibranched C<sub>19</sub> isomers was known from previous

	Example of branching configuration	Position of broken C-C bounds	Type of cracked product
<b>A</b>		Next to outer methyl group	Linear and tribranched fragments
<b>B</b>		Next to inner methyl group	Monobranched and dibranched fragments
<b>C</b>		Next to inner methyl group	Monobranched and dibranched fragments
<b>D</b>		Next to inner methyl group (shifted to same position as outer methyl group)	Monobranched and dibranched fragments

**Fig. 7.** Hydrocracking pathways of tetramethylpentadecanes leading to linear plus tribranched fragment via cleavage of carbon–carbon bond next to outer methyl branching (A) and to monobranched plus dibranched fragments via cleavage of carbon–carbon bond next to inner methyl branching (B–D).



**Fig. 8.** Ratio of the sum of yields of monobranched plus dibranched cracked products to linear plus tribranched cracked products against hydrocracking conversion of pristane on Pt/SiO<sub>2</sub>-Al<sub>2</sub>O<sub>3</sub> (■) and Pt/US-Y zeolite (▲) catalysts. Reaction conditions of Figs. 2 and 12.

work [31,32]. Such isomers were not formed. Tribranched and tetrabranched *i*-C<sub>19</sub> isomers probably could not be separated on the GC column. The evidence for absence of changes of branchiness (Table 2) led us to assume that the pristane skeletal isomers were tetrabranched.

Based on the experience with elution sequences of mono-branched and dibranched long-chain *n*-alkanes [31,32], the fraction eluting later than pristane was assumed to represent isomers with one or two methyl groups at a C<sub>3</sub> positions. Isomers eluting earlier than pristane were considered to have one or both inner methyl branchings shifted (Fig. 9). Based on this tentative assignment, on the silica–alumina catalyst, most of the isomers had a shifting of central methyl branching, especially at low conversion (Fig. 10). It was already discussed that alkylcarbenium ions derived from the pristane molecule with positive charge at C<sub>8</sub> were little sensitive to type C hydrocracking (Fig. 4C). Through methyl

shifting, the two most central methylbranchings can be grouped to enable a type B<sub>2</sub> hydrocracking (Fig. 10). Methyl shifting of the two middle methyl branches according to the GC analysis of the C<sub>19</sub> skeletal isomers was more abundant than shifting of the methyl groups on C<sub>2</sub> to C<sub>3</sub> positions (Fig. 11). The preferred shifting of the middle methyl groups could offer a tentative explanation why the splitting the pristane molecule into a C<sub>9</sub> and a C<sub>10</sub> piece was one of the preferred scission modes (Fig. 3A–F).

### 3.2. Hydroconversion of pristane over Pt/US-Y zeolite

Pristane was also converted over a commercial ultrastable Y zeolite loaded with platinum (Pt/US-Y). The pristane conversion and the yield of skeletal isomers and cracked products were plotted against reaction temperature in Fig. 12. On the Pt/US-Y zeolite, there was less skeletal isomerization of pristane compared to Pt/SiO<sub>2</sub>-Al<sub>2</sub>O<sub>3</sub> catalyst (Fig. 12 compared to Fig. 2). On Pt/US-Y, the pristane skeletal isomerization conversion reached a maximum of ca. 55% around 240 °C. The hydrocracking conversion increased steadily with reaction temperature.

The distribution of skeletal isomers according to the presence or absence of a methylbranching at C<sub>3</sub> position is presented in Fig. 13. On the Pt/US-Y catalyst, the formation of tetrabranched isomers with and without methyl group at C<sub>3</sub> carbons proceeded in parallel. In this respect, the Pt/US-Y catalyst was different from Pt/SiO<sub>2</sub>-Al<sub>2</sub>O<sub>3</sub> which favored positional shifting of the more central methyl branches (Fig. 11).

The hydrocracked products were analyzed for carbon numbers and branchiness (Fig. 14). The peculiarities in the cracked product distribution observed with Pt/SiO<sub>2</sub>-Al<sub>2</sub>O<sub>3</sub> catalyst especially at low hydrocracking conversion (Fig. 3A) were also present on Pt/US-Y (Fig. 14A): (i) absence of propane; (ii) abundant formation of C<sub>6</sub>

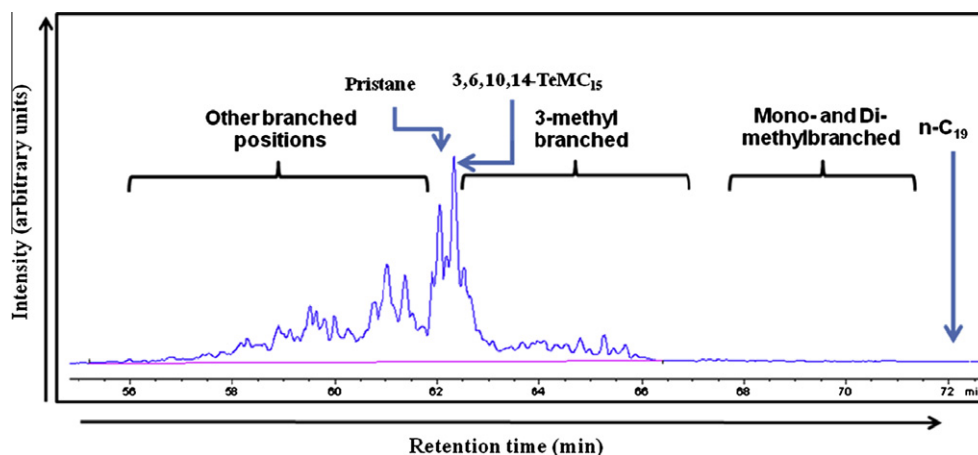


Fig. 9. Example of chromatogram of skeletal isomers of pristane obtained over Pt/SiO<sub>2</sub>-Al<sub>2</sub>O<sub>3</sub> catalyst.

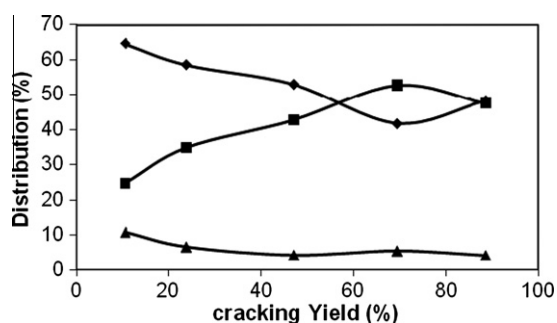


Fig. 10. Distribution of pristane (▲) and its skeletal isomers (%) obtained on Pt/SiO<sub>2</sub>-Al<sub>2</sub>O<sub>3</sub> catalyst according to the presence (■) or absence (◆) of a methyl branching at C<sub>3</sub>. Reaction conditions of Fig. 2.

products, almost all monobranched; and (iii) formation of a C<sub>5</sub> fraction with significant *n*-C<sub>5</sub> content.

At low conversion, the formation of light products (C<sub>4</sub>-C<sub>6</sub>) due to secondary cracking was very pronounced on Pt/US-Y. Like on the Pt/SiO<sub>2</sub>-Al<sub>2</sub>O<sub>3</sub> catalyst, once a pristane molecule started cracking, the primary fragment cracked a second time explaining the formation of *n*-C<sub>5</sub> (Fig. 6). Secondary cracking was significant at low hydrocracking conversion levels (Table 3). The cracked products were analyzed for branchiness (Table 3). On the Pt/US-Y catalyst, the branchiness of the cracked products was around 1.4–1.5 corresponding to cracking reactions of tetrabranched molecules without change of branching degree. The selectivity for cracking next to inner versus outer methyl side chains was analyzed as done for the Pt/SiO<sub>2</sub>-Al<sub>2</sub>O<sub>3</sub> catalyst (Fig. 8). The two catalysts behaved very similarly at low hydrocracking yield. At higher hydrocracking levels, the zeolite maintained a selectivity ratio of around six times cracking near inner branching for one cracking near outer methyl branchings, while the silica–alumina displayed a decreasing trend. The less pronounced skeletal isomerization on the zeolite compared to the silica–alumina (Figs. 2 and 12) offers an explanation why the imprint of the original branching configuration of the pristane molecule is preserved at higher conversion.

Presently, we do not know why certain modes of skeletal isomerization and hydrocracking are suppressed compared to others and can only speculate. The two investigated catalysts, Pt/SiO<sub>2</sub>-Al<sub>2</sub>O<sub>3</sub> and Pt/US-Y, are ideal bifunctional catalysts in the conversion of *n*-alkanes, with skeletal isomerization and hydrocracking occurring as consecutive reactions and hydrocracking via all possible β-scission modes. In the conversion of pristane, the occurrence of secondary cracking at low cracking conversion (221 mol cracked

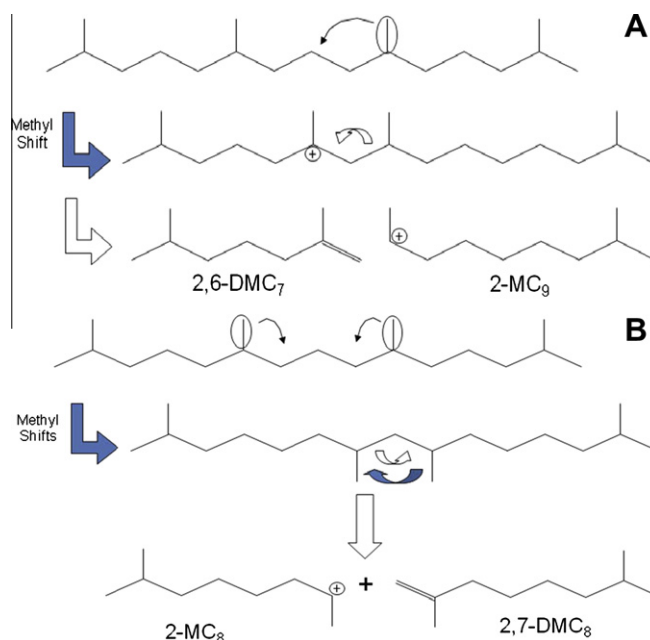
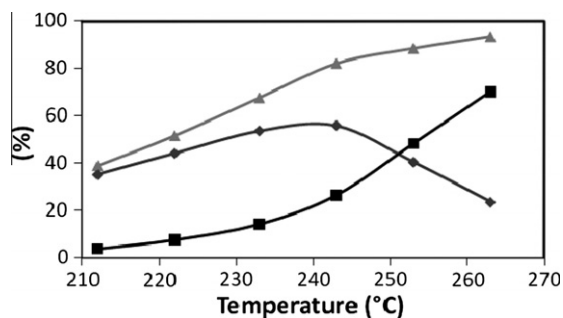


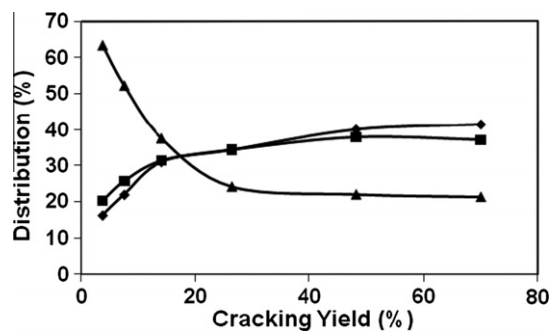
Fig. 11. Examples of reaction pathways leading to the cracking of pristane into C<sub>9</sub> and C<sub>10</sub> fragments. Positive charges are omitted when two possibilities are present.

products/100 mol pristane cracked at 4.9% hydrocracking conversion on Pt/SiO<sub>2</sub>-Al<sub>2</sub>O<sub>3</sub>, Table 2, and 217 mol cracked products/100 mol pristane cracked at 7.5% hydrocracking conversion on Pt/US-Y, Table 3) is typical for catalysts in which the hydrogenation–dehydrogenation function and the acid function are not well balanced. The special hydrocracking product pattern obtained with pristane was most pronounced at these low hydrocracking conversion levels. One possible explanation is that the formation of alkylcarbenium ions having a positively charged C atom near the center of the pristane molecule is suppressed. Protonation at such position is needed, e.g., for the type C hydrocracking mode leading to C<sub>8</sub> and C<sub>11</sub> products according to the reaction scheme of Fig. 4C. Dehydrogenation and formation of C=C double bonds near the center of a tetrabranched C<sub>19</sub> molecule by dehydrogenation on the Pt particles of the catalyst might be suppressed, or else the positional shifting of the positive charge along the chain by hydride shift. However, the abundant occurrence of skeletal isomerization (Fig. 2) and the preferred positional changes of the two central methyl groups (Fig. 10) necessitate protonation of the molecule at C atom positions next to those inner methyl groups. It is an argu-





**Fig. 12.** Conversion (▲), and hydroisomerization (◆) and hydrocracking (■) yield from pristane versus reaction temperature (°C) on Pt/US-Y zeolite. Reaction conditions:  $W/F_0 = 1700$  kg s/mol.,  $P_{\text{tot}} = 0.45$  MPa;  $P_{\text{H}_2/\text{HC}} = 13.1$ .

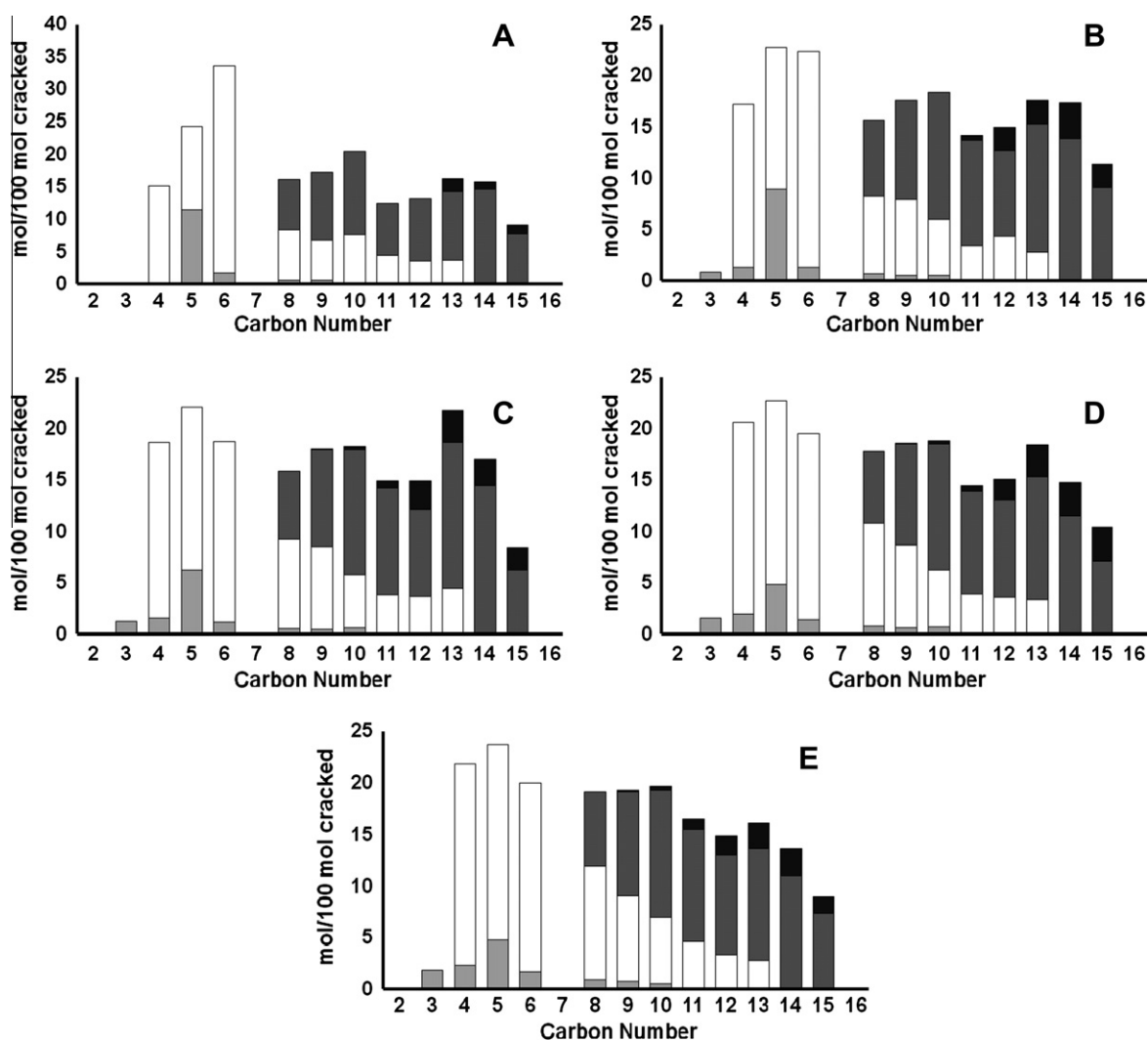


**Fig. 13.** Distribution of pristane (▲) and its skeletal isomers with (■) or without (◆) methyl branching at C<sub>3</sub> position against hydrocracking yield on Pt/US-Y zeolite. Reaction conditions of Fig. 12.

ment against a suppression of protonation near the center of the pristane molecule.

In a  $\beta$ -scission reaction, the positive charge is transferred to a C atom two positions away from the original position. It can be speculated that certain  $\beta$ -scissions might be suppressed for sterical reasons when a too large separation of the positive charge on the

hydrocarbon and negative charge on the catalyst surface would be involved. Similar phenomena have been observed in pore mouth catalysis on Pt/ZSM-22 zeolite, where  $\beta$ -scission reactions of branched alkylcarbenium ions leading to fragments carrying the positive charge outside of the zeolite pore have been found



**Fig. 14.** Cracked product distributions from pristane on Pt/US-Y catalyst at different reaction temperatures. Each fraction is divided according to branchiness: light gray: linear; white: monobranched; dark gray: dibranched; black: tribranched. Reaction temperature and hydrocracking yields: (A) 222 °C, 7.5%; (B) 233 °C, 14.2%; (C) 243 °C, 26.4%; (D) 253 °C, 48.2%; (E) 263 °C, 70.1%. Reaction conditions of Fig. 12.

**Table 3**  
Branchiness of hydrocracked products from pristane on Pt/US-Y catalyst.

Experimental condition	T (°C)	Hydrocracking yield		Average branchiness of cracked products	
		%	Mol/100 mol pristane cracked	Experimental	In absence of change of branchiness <sup>a</sup>
A	222	7.5	217	1.5	1.4
B	233	14.2	209	1.4	1.4
C	243	26.4	208	1.4	1.4
D	253	48.2	212	1.4	1.4
E	263	70.1	216	1.4	1.4

<sup>a</sup> Assuming absence of changes of branchiness of pristane skeletal isomers undergoing.

to be suppressed [36,37]. Molecular modeling efforts will be needed to evaluate the validity of such hypothesis.

#### 4. Conclusions

Pristane (2,6,10,14-tetramethylpentadecane) is a convenient model molecule for investigating hydrocracking reaction pathways of heavy multibranched alkanes with discarded methylbranched contained in renewable hydrocarbon feedstocks. Analysis of the reaction products from pristane skeletal isomerization and hydrocracking on silica–alumina and ultrastable Y zeolite catalyst revealed a peculiar selectivity. Both catalysts caused methyl shifts but did not alter the degree of branching of the tetrabranched pristane molecule. The zeolite aselectively altered the position of the four methyl groups along the main chain, while the silica–alumina favored positional shifting of the two inner methyl groups. On both catalysts at low hydrocracking conversion, one specific hydrocracking pathway leading to 2-methylpentane and 2,6-dimethylundecane was strongly favored. This hydrocracking reaction can be explained by type C (sec → sec) β-scission of an alkylcarbenium ion charged at C<sub>4</sub> derived from the pristane molecule. Even at low hydrocracking conversion, the primary 2,6-dimethylundecane fragment underwent another cracking into *n*-pentane and 2-methylheptane. At higher conversions, the fingerprint of pristane in the cracked products was less apparent because of skeletal isomerization. On both catalysts, the hydrocracking occurred preferentially at carbon–carbon bonds next to the inner methylbranchings leading to a monobranched and a dibranched fragment. This investigation revealed that kinetic models for hydrocracking of linear alkanes in which scissions of alkylcarbenium ions of a same type are considered to occur at a same rate will be inadequate for a description of hydrocracking of heavy multibranched isomers. Pristane can serve as a new paradigm for that type of catalytic chemistry.

#### Acknowledgment

J.A.M. acknowledges the Flemish government for long-term structural funding (Methusalem).

#### References

[1] J. Scherzer, A.J. Gruia, in: M. Dekker (Ed.), *Hydrocracking Science and Technology*, 1996.

- [2] J.A.R. van Veen, J.K. Minderhoud, L.G. Huve, W.H.J. Stork, *Hydrocracking and Catalytic Dewaxing, Handbook of Heterogeneous Catalysis*, 2008, p. 2778.
- [3] M. Stöcker, *Angew. Chem. Int. Ed.* 47 (2008) 9200.
- [4] D. Hayes, *Catal. Today* 145 (2009) 138.
- [5] M. Höök, *Int. J. Energy Res.* 34 (2010) 848.
- [6] P. Courty, J.F. Gruson, *Oil Gas Sci. Technol.* 56 (2001) 515.
- [7] A. de Klerk, *Green Chem.* 10 (2008) 1249.
- [8] N.H. Tran, J.R. Bartlett, *Fuel* 89 (2010) 265.
- [9] L.W. Hillen, G. Pollard, L.V. Wake, N. White, *Biotechnol. Bioeng.* 24 (1982) 193.
- [10] C. Dayananda, R. Sanada, V. Kumar, *Electr. J. Biotechnol.* 10 (1) (2007).
- [11] P. Metzger, C. Largeau, *Appl. Microbiol. Biotechnol.* 66 (2005) 486.
- [12] J. Weitkamp, *Ind. Eng. Chem. Res. Dev.* 21 (1982) 550.
- [13] J.A. Martens, P.A. Jacobs, in: J.B. Moffat (Ed.), *Theoretical Aspects of Heterogeneous Catalysis*, Van Nostrand Reinhold, New York, 1990, p. 52.
- [14] J.A. Martens, P.A. Jacobs, J. Weitkamp, *Appl. Catal.* 20 (1986) 239.
- [15] J.A. Martens, P.A. Jacobs, in: E.G. Derouane (Ed.), *Zeolite Microporous Solids: Synthesis, Structure, and Reactivity*, Kluwer Academic, 1993, p. 511.
- [16] J.A. Martens, P.A. Jacobs, *J. Catal.* 124 (1990) 357.
- [17] J. Weitkamp, P.A. Jacobs, J.A. Martens, *Appl. Catal.* 8 (1983) 123.
- [18] M. Steijns, G.F. Froment, P.A. Jacobs, J.B. Uytterhoeven, J. Weitkamp, *Ind. Eng. Chem. Prod. Res. Dev.* 20 (1981) 654.
- [19] M. Steijns, G.F. Froment, *Ind. Eng. Chem. Res. Dev.* 20 (1981) 660.
- [20] M.A. Baltanas, H. Vansina, G. Froment, *Ind. Eng. Chem. Prod. Res. Dev.* 22 (1983) 532.
- [21] J.A. Martens, M. Tielen, P.A. Jacobs, *Catal. Today* 1 (1987) 435.
- [22] J.A. Martens, P.A. Jacobs, J. Weitkamp, *Appl. Catal.* 20 (1986) 283.
- [23] M. Steijns, G.F. Froment, P.A. Jacobs, J.B. Uytterhoeven, J. Weitkamp, *Erdöl Kohle Erdgas Petrochem.* 31 (1978) 581.
- [24] J.A. Martens, M. Tielen, P.A. Jacobs, in: H.G. Karge, J. Weitkamp (Eds.), *Zeolites as Catalysts, Sorbents and Detergent Builders*, Stud. Surf. Sci. Catal., Elsevier Science Publishers B.V., Amsterdam, 1989, p. 51.
- [25] J.W. Thybaut, I.R. Choudhury, J.F. Denayer, G.V. Baron, P.A. Jacobs, J.A. Martens, *Top. Catal.* 52 (2009) 1251.
- [26] J. Avignan, M. Blumer, *J. Lipid Res.* 9 (1968) 350.
- [27] B. Valderrama, *Stud. Surf. Sci. Catal.* 151 (2004) 373.
- [28] R.J. Taylor, R.H. Petty, *Appl. Catal. A: Gen.* 119 (1994).
- [29] K.P. de Jong, J. Zečević, H. Friedrich, P.E. de Jongh, M. Bulut, S. van Donk, R. Kennogne, A. Finiels, V. Hulea, F. Fajula, *Angew. Chem. Int. Ed.* 12 (2010) 10272.
- [30] E. Valery, D. Guillaume, K. Surla, P. Galtier, J. Verstraete, D. Schweich, *Ind. Eng. Chem. Res.* 46 (2007) 4755.
- [31] M.C. Claude, J.A. Martens, *J. Catal.* 190 (2000) 39.
- [32] M.C. Claude, G. Vanbutsele, J.A. Martens, *J. Catal.* 203 (2001) 213.
- [33] G. Hastoy, E. Guillon, J.A. Martens, *Stud. Surf. Sci. Catal.* 158B (2005) 1359.
- [34] G.G. Martens, G.B. Marin, J.A. Martens, P.A. Jacobs, G.V. Baron, *J. Catal.* 195 (2000) 253.
- [35] J.W. Thybaut, G.B. Marin, G.V. Baron, P.A. Jacobs, J.A. Martens, *J. Catal.* 202 (2001) 324.
- [36] C.S. Laxmi Narasimhan, J.W. Thybaut, G.B. Marin, P.A. Jacobs, J.A. Martens, J.F. Denayer, G.V. Baron, *J. Catal.* 220 (2003) 399.
- [37] W. Souverijns, J.A. Martens, G.F. Froment, P.A. Jacobs, *J. Catal.* 174 (1998) 177.